

Critical behavior and net-charge fluctuations from lattice QCD*

Frithjof Karsch

Fakultät für Physik, Universität Bielefeld, D-33615 Bielefeld, Germany

Physics Department, Brookhaven National Laboratory, Upton, NY 11973, USA

E-mail: karsch@physik.uni-bielefeld.de

We present recent results on the critical and pseudo-critical temperatures in $(2+1)$ -flavor QCD with a physical strange quark mass and two degenerate light quark masses extrapolated to the chiral limit and tuned to the physical value, respectively. We furthermore discuss implication of the observed low chiral phase transition temperature, $T_c^0 = 132_{-6}^{+3}$ MeV, for the structure of cumulants of conserved charge fluctuations at vanishing baryon chemical potential and consequences for the possible location of the QCD critical endpoint in the QCD phase diagram at non-zero baryon chemical potential.

Corfu Summer Institute 2018 "School and Workshops on Elementary Particle Physics and Gravity" (CORFU2018)

31 August - 28 September, 2018

Corfu, Greece

*Based on talks given at the conference "*The Critical Point and Onset of Deconfinement*" (CPOD 2018), Sept. 24-28, 2018, Corfu, Greece; the EMMI workshop "*Probing the Phase Structure of Strongly Interacting Matter: Theory and Experiment*", March 25-29, 2019, GSI Darmstadt, Germany, and the EMMI Rapid Task Force meeting "*Dynamics of critical fluctuations: theory-phenomenology-HIC*", April 8-12, 2019, GSI Darmstadt, Germany.

1. Introduction

Understanding the phase structure of strongly interacting matter is one of the central goals in studies of the properties of strong interaction matter at finite temperature and density through large-scale numerical calculations in the framework of lattice regularized Quantum Chromo Dynamics (QCD). Also experimentally major efforts at the Large Hadron Collider (LHC) at CERN and the Relativistic Heavy Ion Collider (RHIC) at Brookhaven National Laboratory are devoted to this goal.

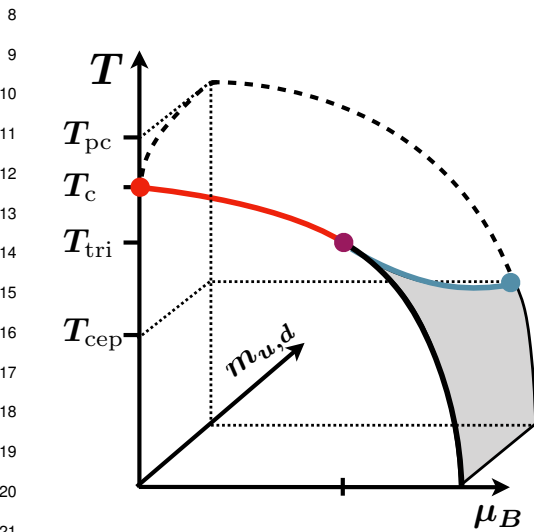


Figure 1: Sketch of a possible QCD phase diagram in the space of temperature (T), baryon chemical potential (μ_B) and light quark masses ($m_{u,d}$).

persists as such also at non-zero baryon chemical potential.

At non-zero values of the two light quark masses the transition is only a smooth crossover for small values of μ_B . At larger μ_B , however, it is expected that a second order phase transition arises at the endpoint (T_{cep}) of a line of first order transitions, at which the net baryon-number density changes discontinuously [4]. Critical behavior in the vicinity of this endpoint will be controlled by the 3-d, $Z(2)$ universality class. This Ising-like transition will exist for arbitrary values of the light quark masses and thus will meet the $O(4)$ chiral transition line at $m_{u,d} = 0$ in a tri-critical point (T_{tri}). A sketch of the resulting phase diagram, which also indicates the relative ordering of the various transition temperatures, is shown in Fig. 1. This generic phase diagram, in particular the indicated ordering of the various characteristic (phase) transition temperatures, is in qualitative agreement with various model calculations [4, 5, 6].

In the following we will present recent lattice QCD results on the pseudo-critical (T_{pc}) and critical temperature (T_c) in $(2+1)$ -flavor QCD at $\mu_B = 0$. We relate these findings to the structure of higher order cumulants of conserved charge fluctuations, and discuss how they constrain the location of a possible critical point at $\mu_B > 0$ and physical values of the quark masses.

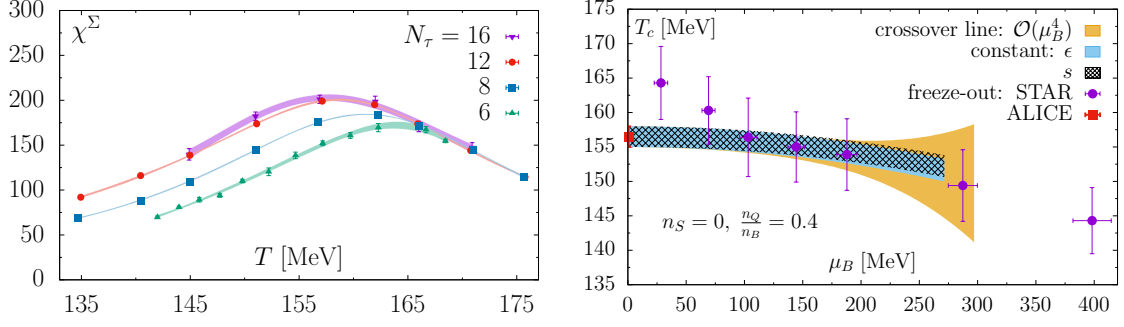


Figure 2: *Left:* The chiral susceptibility ($\chi^\Sigma \equiv \chi_M$) calculated on lattices with different temporal extent N_τ for physical values of the degenerate light (u, d) and strange quark masses. *Right:* Crossover temperature $T_{pc}(\mu_B)$ determined from continuum extrapolated results for the location of peaks in the chiral susceptibilities defined in Eq. 2.2 and some further observables introduced in Ref. [7]. Also shown in this figure are lines of constant energy and entropy density [8] as well as results for freeze-out temperatures determined from data on particle yields measured by the STAR and ALICE collaborations [9, 10].

2. Universal pseudo-critical and critical behavior

2.1 Pseudo-critical temperature in (2+1)-flavor QCD

In the limit of vanishing up and down quark masses QCD possesses an exact global symmetry, the chiral $SU_L(2) \times SU_R(2)$ flavor symmetry. This symmetry is spontaneously broken at low temperature, signaled by a non-vanishing chiral condensate ($\langle \bar{\psi}\psi \rangle$). Chiral symmetry is explicitly broken due to the non-vanishing light quark masses. Nonetheless, this explicit breaking is small enough for chiral symmetry providing a good, approximate order parameter at non-zero temperature – the chiral condensate $\langle \bar{\psi}\psi \rangle$. Its variation with quark mass as well as temperature is large in a small temperature interval, which leads to well defined peaks in the corresponding chiral (χ^Σ) and mixed (χ_i) susceptibilities. These maxima in the susceptibilities are used to define pseudo-critical temperatures, which, in the limit of vanishing quark masses, converge to the uniquely defined critical temperature for the chiral phase transition.

For our studies of the chiral phase transition we use as an order parameter for chiral symmetry breaking

$$\Sigma = \frac{1}{f_K^4} [m_s (\langle \bar{\psi}\psi \rangle_u + \langle \bar{\psi}\psi \rangle_d) - (m_u + m_d) \langle \bar{\psi}\psi \rangle_s], \quad (2.1)$$

where $\langle \bar{\psi}\psi \rangle_f = T(\partial \ln Z / \partial m_f) / V$ denotes chiral condensates of the up (u), down (d), and strange (s) quarks. A fraction of the strange quark chiral condensates is subtracted from the light quark chiral condensates in order to eliminate ultra-violet divergences, linear in the quark masses, and the condensates are multiplied with the strange quark mass in order to define a renormalization group invariant observable. The kaon decay constant f_K is used to set the scale and define a dimensionless order parameter Σ (sometimes also denoted as M).

Pseudo-critical temperatures are extracted from the location of peaks in the chiral and mixed

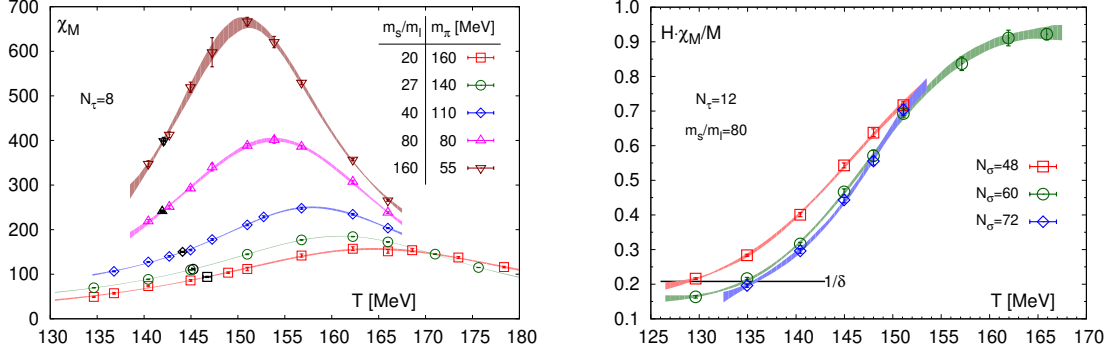


Figure 3: *Left:* The chiral susceptibility for several values of the quark mass ratio $H = m_l/m_s$ on lattices with temporal extent $N_\tau = 8$ and spatial lattice sizes that are varied in the range $N_\sigma = (4 - 7)$ when going from the largest to the smallest light quark mass value. *Right:* The ratio $H\chi_M/M$ for $H = 1/80$ and $N_\tau = 12$ for three different spatial lattice sizes N_σ .

62 susceptibilities

$$\chi_M = m_s \left(\frac{\partial}{\partial m_u} + \frac{\partial}{\partial m_d} \right) \Sigma, \quad (2.2)$$

$$\chi_t = T \frac{d}{dT} \Sigma. \quad (2.3)$$

63 For different values of the lattice spacing, $a = 1/TN_\tau$, the peak locations in different susceptibilities
 64 are determined. From an extrapolation to the continuum limit, that takes into account $\mathcal{O}(a^2)$ cut-
 65 off effects one then determines pseudo-critical temperatures for the chiral transition. Results from
 66 a recent determination of pseudo-critical temperatures at physical values of the light and strange
 67 quark masses are shown in Fig. 2. The left hand figure shows the chiral susceptibility ($\chi^\Sigma \equiv$
 68 χ_M) calculated on different size lattices ($N_\sigma^3 N_\tau$, with $N_\sigma = 4N_\tau$) [7] using the Highly Improved
 69 Staggered Quark (HISQ) action [11]. Other observables, e.g. the mixed susceptibility χ_t , yield
 70 pseudo-critical temperatures, which in the continuum limit differ from each other by less than
 71 2 MeV [7]. For the pseudo-critical temperature this analysis yields,

$$T_{pc} = (156.5 \pm 1.5) \text{ MeV}. \quad (2.4)$$

72 A comparison of this pseudo-critical temperature with the freeze-out temperature determined from
 73 data on particle yields in heavy ion collisions at the LHC [9] suggests that the formation of hadrons
 74 after the cooling of the expanding hot and dense quark-gluon matter created in these collisions
 75 does take place close to the phase boundary characterized by this pseudo-critical temperature (see
 76 Fig. 2 (right)).

77 2.2 Critical temperature in (2+1)-flavor QCD

78 An analogous analysis can be performed for other values of the light quark masses ($m_l \equiv$
 79 $(m_u + m_d)/2$), keeping the strange quark mass fixed at its physical value. The approach to the
 80 chiral limit, $H \equiv m_l/m_s \rightarrow 0$, can then be examined by monitoring the quark mass dependence of
 81 the chiral order parameter and its susceptibility (χ_M). Some results for the quark mass dependence

82 of χ_M , calculated with the HISQ action, are shown in Fig. 3 (left) [12]. For sufficiently small values
 83 of the light quark masses and close to the chiral transition temperature, *i.e.* in the scaling regime,
 84 the peak location in χ_M , and similarly in χ_t , is controlled by universal scaling functions,

$$\chi_M(T, H) \sim h^{1/\delta-1} f_\chi(z) + \text{regular} , \quad \chi_t(T, H) \sim h^{1/\delta-1/\beta\delta} f'_G(z) + \text{regular} , \quad (2.5)$$

85 where β and δ are critical exponents for the universality class of the chiral transition, $z \equiv z_0[(T -$
 86 $T_c^0)/T_c^0]/H^{1/\beta\delta}$, $h = H/h_0$ and h_0, z_0 are non-universal constants. The peak locations in χ_M and χ_t
 87 are related to maxima of the scaling functions $f_\chi(z)$ and $f'_G(z)$, respectively. The quark mass de-
 88 pendence of pseudo-critical temperatures thus is controlled by the scaling variable z . The increase
 89 of the peaks is controlled by the prefactors. As can be seen in Fig. 3 (left) the peak in χ_M increases
 90 rapidly with decreasing quark, or equivalently pion, mass and the peak location shifts towards
 91 smaller values of the temperature. In the scaling regime, close to the chiral limit, contributions
 92 from regular terms will be small and one expects to find

$$T_{pc}(H) = T_c^0 \left(1 + \frac{z_X}{z_0} H^{1/\beta\delta} \right) , \quad (2.6)$$

93 with z_X being a universal constant defining the location of the maximum in χ_X , e.g. $X \equiv M$ or
 94 t when using the peak locations of χ_M and χ_t defined in Eq. 2.2 and Eq. 2.3, respectively. For
 95 the 3- d , $O(4)$ universality class one has, $z_M \simeq 1.4(1)$, $z_t \simeq 0.8(2)$, and $1/\beta\delta \simeq 0.55$ [13]. As z_0
 96 typically is of $\mathcal{O}(1)$, Eq. 2.6 suggests that the pseudo-critical temperatures determined from the
 97 peak locations in χ_M and χ_t will show a rather strong dependence on the light quark masses. In
 98 fact, QCD-inspired model calculations [14, 15] suggest that T_c^0 might be (20 – 30) MeV smaller
 99 than T_{pc} calculated for physical values of the quark masses, for which $H \simeq 1/27$.

100 In order to determine the chiral phase transition temperature T_c^0 it thus would be advantageous
 101 to use observables which similarly to the maxima in susceptibilities correspond to a fixed value of
 102 the scaling variable z , but are related to a value $z \equiv z_X$ that is close to zero. Two such observables
 103 have been utilized recently [12] for this purpose. One may define two characteristic temperatures,
 104 T_δ and T_{60} , through the relations

$$\frac{H\chi_M(T_\delta)}{M(T_\delta)} = \frac{1}{\delta} , \quad (2.7)$$

$$\chi_M(T_{60}) = 0.6\chi_M^{\text{peak}} . \quad (2.8)$$

105 In the thermodynamic limit the corresponding scaling variables z_δ and z_{60} both are close to zero.
 106 The resulting estimators, T_δ and T_{60} , for the chiral phase transition temperature are quark mass
 107 dependent only due to the presence of contributions arising from regular terms in the partition
 108 function. They therefore provide good estimators for the chiral phase transition temperature. Some
 109 results for the ratio $H\chi_M/M$, from which the estimator T_δ is extracted, are shown in Fig. 3 (right).
 110 When decreasing the quark masses towards the chiral limit finite volume effects increase and some
 111 care needs to be taken in the extrapolation to the thermodynamic limit. After (i) infinite volume, (ii)
 112 continuum, and (iii) chiral limit extrapolations these estimators yield for the chiral phase transition
 113 temperature [12]

$$T_c^0 = 132_{-6}^{+3} \text{ MeV} . \quad (2.9)$$

114 The chiral phase transition temperature thus is about 25 MeV smaller than the pseudo-critical
 115 temperature extracted from the location of the peak in the chiral susceptibility. As will be discussed
 116 further in Section 3, this has consequences also for the phase transition temperature T_{cep} at which
 117 a possible critical point at physical values of the light quark masses and at non-zero values of the
 118 baryon chemical potential may occur.

119 2.3 Curvature of the phase transition line in the chiral limit

120 Close to the chiral limit, in the vicinity of the critical temperature, the non-analytic (singular)
 121 behavior of the logarithm of the partition function, *i.e.* the pressure, is described by a scaling
 122 function, $f_s(z)$. Deviations from scaling are given in terms of an analytic (regular) function f_r ,

$$\frac{P}{T^4} = h^{2-\alpha} f_s(z) + f_r(T, \mu_B, \mu_Q, \mu_S, m_f), \quad (2.10)$$

123 The reduced temperature variable t entering the scaling variable $z \sim t/h^{1/\beta\delta}$ will also dependent
 124 on the chemical potentials. In leading order, and for vanishing strangeness and electric charge
 125 chemical potentials, one has

$$t \sim \frac{T - T_c^0}{T_c^0} + \kappa_2^{B,0} \left(\frac{\mu_B}{T} \right)^2, \quad (2.11)$$

126 which also reflects the temperature dependence of the chiral phase transition temperature, $T_c(\mu_B) =$
 127 $T_c^0(1 - \kappa_2^{B,0}(\mu_B/T)^2)$.

128 At physical values of the quark masses the curvature of the transition line, κ_2^B , will in general
 129 differ from $\kappa_2^{B,0}$, receiving corrections from regular terms, terms arising from universal corrections-
 130 to-scaling or higher order terms in the scaling variables being proportional to $H(T - T_c^0)$. This
 131 curvature term can be extracted from the μ_B -dependence of the location of maxima of various
 132 susceptibilities. Using a Taylor expansion of, e.g. the mixed chiral susceptibility $\chi_t(T, \mu_B)$ in terms
 133 of temperature and baryon chemical potential around the pseudo-critical point ($T_{pc}, \mu_B = 0$), one
 134 obtains for the curvature κ_2^B [7],

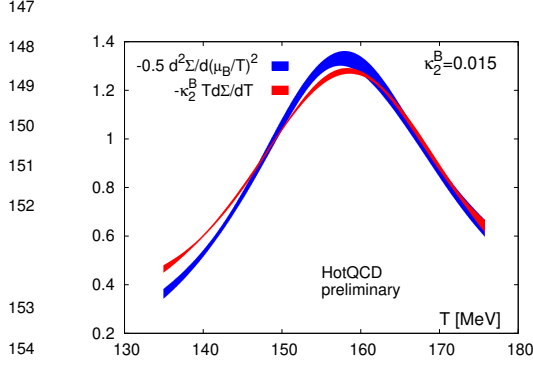
$$\kappa_2^B = \frac{1}{2T^2 \partial_T^2 \chi_t} \left[T \partial_T \chi_t' - 2\chi_t' \right] \Big|_{(T_{pc}, \mu_B=0)}, \quad (2.12)$$

135 with $\chi_t' = T^2 \partial^2 \chi_t / \partial \mu_B^2$. Similarly one can derive expressions for higher order expansion coeffi-
 136 cients of $T_{pc}(\mu_B)$. The analysis performed in Ref. [7] gave $\kappa_2^B = 0.015(4)$ in agreement with other
 137 recent determinations of the leading order correction to T_{pc} [16, 17]. The next-to-leading order
 138 correction, κ_4^B , is an order of magnitude smaller and consistent with zero within current statistical
 139 errors. The resulting μ_B -dependence of the crossover line for physical quark masses is shown in
 140 Fig. 2 (right).

141 In the limit of vanishing quark mass the curvature coefficients κ_2^B will approach the corre-
 142 sponding curvature term of the chiral phase transition line, $\kappa_2^{B,0}$. In fact, in the absence of contri-
 143 butions from regular terms the curvature coefficient will be quark mass independent, as seen from
 144 the general scaling ansatz given in Eq. 2.10. To what extent this holds true may be probed by
 145 comparing temperature and chemical potential derivatives of P/T^4 . In the absence of substantial

146 contributions from regular terms one expects to find in the scaling regime,

$$\frac{T^2}{2} \frac{\partial^2 \Sigma}{\partial \mu_B^2} = \kappa_2^{B,0} T_c^0 \frac{\partial \Sigma}{\partial T}. \quad (2.13)$$



155 **Figure 4:** Derivatives of the chiral order parameter
156 with respect to temperature and baryon chemical po-
157 tentials, respectively. Shown are results for $N_\tau = 12$.

158
159
160
161 the quark masses is located at a temperature T_{cep} below the chiral phase transition temperature T_c^0 .
162 If this is correct, it has significant consequences also for the properties of higher order cumulants
163 of conserved charge fluctuations.

164 Cumulants of conserved charge fluctuations, evaluated at vanishing chemical potentials ($\mu_{B,Q,S}$),
165 appear as expansion coefficients in Taylor series for thermodynamic quantities. The relative mag-
166 nitude of subsequent expansion coefficients controls the convergence of these expansions and de-
167 termines their radius of convergence. The pattern of sign changes in these expansion coefficients
168 provides information on the location of singularities in the plane of complex-valued chemical po-
169 tentials which cause the breakdown of the Taylor expansions. E.g., for a series of the form $\sum_x c_n x^n$
170 the singularity determining the radius of convergence lies on the real-x axis, if an n_0 exists such
171 that all expansion coefficients c_n are positive for all $n > n_0$ [18] (see also discussion in [19]). Only
172 in this case the radius of convergence can be unambiguously related to the existence of a phase
173 transition in the thermodynamic system under consideration. One thus may examine the sign of
174 subsequent expansion coefficients and their relative magnitude in order to judge whether or not
175 the convergence of a Taylor series is limited by the appearance of a phase transition for some
176 real-valued chemical potential.

177 At small values of the chemical potentials the QCD partition function may be expanded in a
178 Taylor series. E.g. the pressure can be written as

$$\frac{P}{T^4} = \frac{1}{VT^3} \ln Z(T, V, \hat{\mu}_u, \hat{\mu}_d, \hat{\mu}_s) = \sum_{i,j,k=0}^{\infty} \frac{\chi_{ijk}^{BQS}}{i!j!k!} \hat{\mu}_B^i \hat{\mu}_Q^j \hat{\mu}_S^k, \quad (3.1)$$

A test of this relation is shown in Fig. 4, where $\kappa_2^{B,0} \equiv \kappa_2^B$ has been assumed. This indeed suggests that the curvature of the chiral phase transition line is similar in magnitude to that of the pseudo-critical line at physical values of the quark masses.

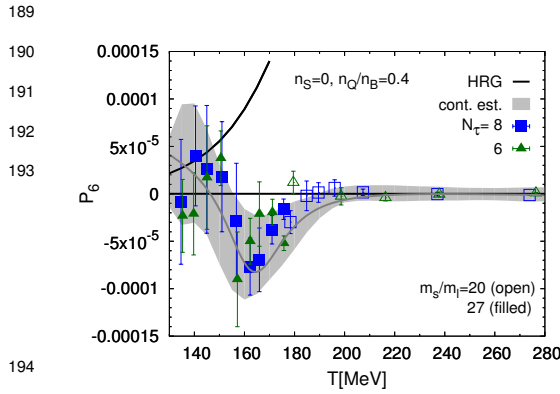
3. Higher order cumulants in the crossover region

The sketch of the QCD phase diagram shown in Fig. 1, which qualitatively is consistent with model calculations for the quark mass dependence of transition lines in the QCD phase diagram [4, 5, 6], suggests that a possible critical point at physical values of

179 with $\chi_{000}^{BQS} \equiv P(T, 0)/T^4$ and $\hat{\mu}_X = \mu_X/T$. The generalized susceptibilities are given as derivatives
 180 of P/T^4 at vanishing values of the conserved charge chemical potentials,

$$\chi_{ijk}^{BQS} \equiv \chi_{ijk}^{BQS}(T) = \left. \frac{\partial P(T, \hat{\mu})/T^4}{\partial \hat{\mu}_B^i \partial \hat{\mu}_Q^j \partial \hat{\mu}_S^k} \right|_{\hat{\mu}=0}. \quad (3.2)$$

181 If, at some value of the temperature, the radius of convergence of the Taylor series for the
 182 pressure arises from a singularity in the complex- μ plane, one should find that Taylor expansion
 183 coefficients will have an irregular sign structure, *i.e.* at this temperature positive and negative
 184 expansion coefficients will appear in the Taylor series. Such changes of sign are indeed observed for
 185 various cumulants of conserved charge fluctuations, starting with sixth order expansion coefficients.
 186 Although not rigorous in the mathematical sense stated above, these sign changes suggest that
 187 Taylor expansions in this temperature range are not limited by a physical singularity related to a
 188 phase transition, but by some singularity in the complex- μ plane.



194
 195
 196 **Figure 5:** Temperature dependence of the sixth order
 197 expansion coefficient of the pressure in (2+1)-flavor
 198 QCD at vanishing net strangeness and fixed electric
 199 charge to baryon number density, $n_Q/n_B = 0.4$ [8].

In Fig. 5 we show the sixth order expansion
 coefficient of the pressure for the case of van-
 ishing net strangeness and a fixed electric
 charge to baryon-number density, $n_Q/n_B =$
 0.4 [8],

$$\frac{P}{T^4} = P_0 + P_2 \hat{\mu}_B^2 + P_4 \hat{\mu}_B^4 + P_6 \hat{\mu}_B^6 + \mathcal{O}(\hat{\mu}_B^8). \quad (3.3)$$

While the expansion coefficients up to
 $\mathcal{O}(\mu_B^4)$ are all positive [8], the sixth order
 expansion coefficient, P_6 , starts to change
 sign with increasing temperature, *i.e.* $P_6 < 0$
 for $T \gtrsim 150$ MeV. These sign changes are ex-
 pected to become more frequent and start at
 lower temperatures in higher orders of the
 expansion.

202 The irregular sign structure becomes more apparent in simpler cumulants like the net up-quark-
 203 number cumulants, which are statistically easier to control. Up to eight order cumulants are shown
 204 in Fig. 6 (left). As can be seen, the sign of $\chi_{n+2}^u(T)$ can be deduced from the temperature derivative
 205 of $\chi_n^u(T)$, as suggested by Eq. 2.11. Similar behavior is found for the expansion coefficients of the
 206 quadratic net electric charge fluctuations at non-zero baryon chemical potential,

$$\chi_2^Q(T, \mu_B) = \chi_{02}^{BQ}(T) + \frac{1}{2} \chi_{22}^{BQ}(T) \hat{\mu}_B^2 + \frac{1}{24} \chi_{42}^{BQ}(T) \hat{\mu}_B^4 + \mathcal{O}(\mu_B^6), \quad (3.4)$$

207 where, for simplicity, we have set $\mu_Q = \mu_S = 0$. The first three expansion coefficients are shown
 208 in Fig. 6 (right). We note that χ_{42}^{BQ} vanishes at the temperature where χ_{22}^{BQ} has its maximum.
 209 Also these expansion coefficients thus seem to be in accordance with the pattern resulting from
 210 Eq. 2.11 in the scaling regime, *i.e.* two derivatives with respect to the baryon chemical potential
 211 are proportional to a single derivative with respect to temperature. This leads to the expectation

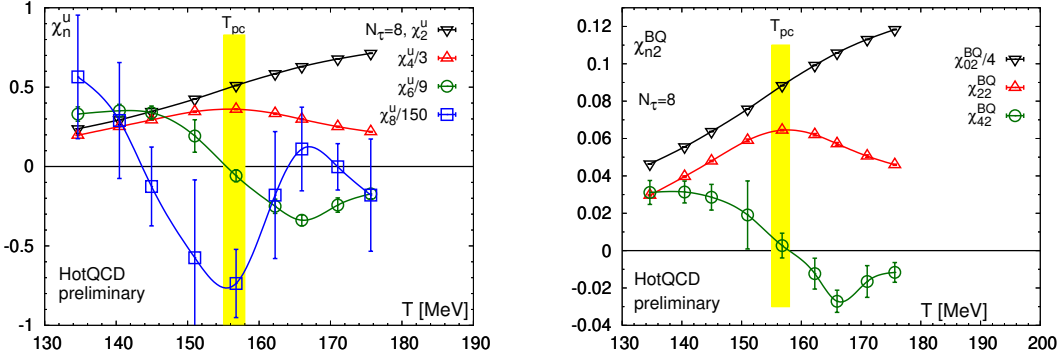


Figure 6: *Left:* Temperature dependence of up to eight order cumulants of net up-quark-number fluctuations calculated on lattices with temporal extent $N_\tau = 8$ *Right:* Expansion coefficients of net electric charge fluctuations for the case of vanishing electric charge and strangeness chemical potentials. In both figures the lines are smooth spline interpolations drawn to guide the eye.

212 that the eight order cumulants, χ_{62}^{BQ} , will be negative in the temperature range $T \in [135 \text{ MeV} :$
 213 $165 \text{ MeV}]$. At high temperature subsequent expansion coefficients thus show an irregular sign
 214 structure, which is in accordance with the expectation that for physical quark mass values a possible
 215 critical endpoint in the QCD phase diagram will be located at a temperature below the chiral phase
 216 transition temperature T_c^0 .

217 4. Conclusions

218 New results on the chiral phase transition temperature T_c^0 in (2+1)-flavor QCD suggests that
 219 this temperature is well below the pseudo-critical temperature T_{pc} at physical values of the light
 220 and strange quark masses. Moreover, it is found that many 6th and higher order cumulants of
 221 conserved charge fluctuations are no longer strictly positive but start showing an irregular sign
 222 structure at temperatures $T \gtrsim T_c^0$. This suggests that a possible second order phase transition at
 223 physical values of the quark masses and for non-vanishing baryon chemical potential can occur
 224 only at a temperature $T_{cep} < T_c^0$, if it exists at all.

225 Acknowledgement

226 This work was supported in part through Contract No. DE-SC001270 with the U.S. Depart-
 227 ment of Energy, the Deutsche Forschungsgemeinschaft (DFG) through the CRC-TR 211 "Strong-
 228 interaction matter under extreme conditions", grant number 315477589 - TRR 211, and the grant
 229 05P18PBCA1 of the German Bundesministerium für Bildung und Forschung.

230 References

- 231 [1] H.-T. Ding, F. Karsch and S. Mukherjee, *Thermodynamics of strong-interaction matter from Lattice*
 232 *QCD, Int. J. Mod. Phys. E24* (2015) 1530007 [1504.05274].
 233 [2] M. D'Elia, *High-Temperature QCD: theory overview, Nucl. Phys. A982* (2019) 99 [1809.10660].
 234 [3] R. D. Pisarski and F. Wilczek, *Remarks on the Chiral Phase Transition in Chromodynamics, Phys.*
 235 *Rev. D29* (1984) 338.

- 236 [4] A. M. Halasz, A. D. Jackson, R. E. Shrock, M. A. Stephanov and J. J. M. Verbaarschot, *On the phase*
 237 *diagram of QCD*, *Phys. Rev.* **D58** (1998) 096007 [hep-ph/9804290].
- 238 [5] M. A. Stephanov, *QCD critical point and complex chemical potential singularities*, *Phys. Rev.* **D73**
 239 (2006) 094508 [hep-lat/0603014].
- 240 [6] M. Buballa and S. Carignano, *Inhomogeneous chiral phases away from the chiral limit*, *Phys. Lett.*
 241 **B791** (2019) 361 [1809.10066].
- 242 [7] A. Bazavov et al., *Chiral crossover in QCD at zero and non-zero chemical potentials*, 1812.08235.
- 243 [8] A. Bazavov et al., *The QCD Equation of State to $\mathcal{O}(\mu_B^6)$ from Lattice QCD*, *Phys. Rev.* **D95** (2017)
 244 054504 [1701.04325].
- 245 [9] A. Andronic, P. Braun-Munzinger, K. Redlich and J. Stachel, *Decoding the phase structure of QCD*
 246 *via particle production at high energy*, *Nature* **561** (2018) 321 [1710.09425].
- 247 [10] STAR collaboration, L. Adamczyk et al., *Bulk Properties of the Medium Produced in Relativistic*
 248 *Heavy-Ion Collisions from the Beam Energy Scan Program*, *Phys. Rev.* **C96** (2017) 044904
 249 [1701.07065].
- 250 [11] HPQCD, UKQCD collaboration, E. Follana, Q. Mason, C. Davies, K. Hornbostel, G. P. Lepage,
 251 J. Shigemitsu et al., *Highly improved staggered quarks on the lattice, with applications to charm*
 252 *physics*, *Phys. Rev.* **D75** (2007) 054502 [hep-lat/0610092].
- 253 [12] H. T. Ding et al., *The chiral phase transition temperature in (2+1)-flavor QCD*, 1903.04801.
- 254 [13] J. Engels and F. Karsch, *The scaling functions of the free energy density and its derivatives for the 3d*
 255 *O(4) model*, *Phys. Rev.* **D85** (2012) 094506 [1105.0584].
- 256 [14] J. Berges, D. U. Jungnickel and C. Wetterich, *Two flavor chiral phase transition from nonperturbative*
 257 *flow equations*, *Phys. Rev.* **D59** (1999) 034010 [hep-ph/9705474].
- 258 [15] J. Braun, B. Klein, H. J. Pirner and A. H. Rezaeian, *Volume and quark mass dependence of the chiral*
 259 *phase transition*, *Phys. Rev.* **D73** (2006) 074010 [hep-ph/0512274].
- 260 [16] R. Bellwied, S. Borsanyi, Z. Fodor, J. Günther, S. D. Katz, C. Ratti et al., *The QCD phase diagram*
 261 *from analytic continuation*, *Phys. Lett.* **B751** (2015) 559 [1507.07510].
- 262 [17] C. Bonati, M. D’Elia, F. Negro, F. Sanfilippo and K. Zambello, *Curvature of the pseudocritical line in*
 263 *QCD: Taylor expansion matches analytic continuation*, *Phys. Rev.* **D98** (2018) 054510
 264 [1805.02960].
- 265 [18] S. Gaunt and A. Gutmann, *Phase Transitions and Critical Phenomena 3 (Edts. C. Domb and M.S.*
 266 *Green)*, *Academic Press* (1974).
- 267 [19] C. R. Allton, M. Doring, S. Ejiri, S. J. Hands, O. Kaczmarek, F. Karsch et al., *Thermodynamics of two*
 268 *flavor QCD to sixth order in quark chemical potential*, *Phys. Rev.* **D71** (2005) 054508
 269 [hep-lat/0501030].